Elastic fracture in random materials

Paul D. Beale
Department of Physics, University of Colorado at Boulder, Campus Box 390, Boulder, Colorado, 80309-0390

David J. Srolovitz*
Los Alamos National Laboratory, Los Alamos, New Mexico 87545
(Received 16 July 1987)

We analyze a simple model of elastic failure in randomly inhomogeneous materials such as minerals and ceramics. We study a two-dimensional triangular lattice with nearest-neighbor harmonic springs. The springs are present with probability p. The springs can only withstand a small strain before they fail completely and irreversibly. The applied breakdown stress in a large, but finite, sample tends to zero as the fraction of springs in the material approaches the rigidity percolation threshold. The average initial breakdown stress, σ_b, behaves as $\sigma_b^{\mu} \approx [A(p)+B(p)\ln(L)]^{-1}$, where L is the linear dimension of the system and the exponent μ is between 1 and 2. The coefficient $B(p)$ diverges as p approaches the rigidity percolation threshold. The breakdown-stress distribution function $F_L(\sigma)$ has the form $F_L(\sigma) \approx 1-\exp[-cL^2\exp(-k/\sigma^{\mu})]$. The parameters c and k are constants characteristic of the microscopic properties of the system. The parameter k tends to zero at the rigidity percolation threshold. These predictions are verified by computer simulations of random lattices. The breakdown process can continue until a macroscopic elastic failure occurs in the system. The failure occurs in two steps. First, a number of springs fail at approximately the strain which causes the initial failure. This results in a system which has zero elastic modulus. Finally, at a considerably larger strain a macroscopic crack forms across the entire sample.

I. INTRODUCTION

The fracture of brittle materials at stresses far below the theoretical strength of the material is usually attributable to the presence of defects, often in the form of microcracks. In Griffith's theory of brittle fracture,[1] the failure of a macroscopic sample occurs when the stress around the largest and/or least favorably oriented crack reaches a critical value. At the critical stress level, the crack propagates unstably through the sample. The value of the applied load at which this occurs depends sensitively on the crack size, orientation, geometry, and local environment. While the individual crack properties can be dealt with in the framework of classical fracture mechanics,[2] the local environments are complicated by the fact that different cracks interact through their slowly decaying strain fields. It is therefore unreasonable to assume that each defect is affected by the same loading. We explicitly abandon this assumption by constructing a random elastic model of failure. Microcracks are distributed randomly in the model system. An external load is applied and the stress and strain are determined throughout the sample. A local fracture criterion is used to model the crack growth problem. Similar methods have been used to describe dielectric breakdown in metal-loaded dielectrics,[3] random fuse networks,[4,5] and crack propagation in random materials.[6]

The model we use is composed of masses on a two-dimensional triangular lattice connected to their nearest neighbors by harmonic springs. The springs are present with probability p and are absent with probability $1-p$. The linear bulk elastic properties of systems of this type have been studied by a number of authors.[7-9] In particular, if p is less than the rigidity percolation threshold[7,8] p_r, Young's modulus vanishes even though a connected path of springs may exist across the system. By contrast, we would like to address nonlinear questions associated with the manner in which these models fracture under the application of an externally applied stress. This analysis yields a new prediction for the failure strengths of random brittle materials such as ceramics, amalgamates, and sintered powders.

In this paper we analyze this simple model of elastic failure by means of theoretical scaling arguments and numerical solution of the elastic equations in a random system. Several important new results are derived from this analysis. As expected, we find that the breakdown stress in the system is sensitive to the fraction of missing springs in the system. This is caused by the formation of clusters of missing springs in the system. The initial failure in the system will occur adjacent to the critical defect, i.e., the largest and/or least favorably oriented defect in the system. The failure or fracture stress is of order an inverse power of the linear dimension of the critical defect. Due to this effect, the breakdown stress tends to zero in the limit as p approaches the rigidity percolation threshold. By contrast, Chakrabarti *et al.*[6] use a Lennard-Jones model for the interaction of the atoms in the solid under stress. They find for their model that the failure stress goes to zero at the normal percolation threshold p_c rather than at the rigidity percolation threshold as we find. This is understandable since in the

Lennard-Jones model no two particles are tied to each other, as is the case with our spring model.

The breakdown stress in our model has an intrinsic size dependence. Large samples of material are more sensitive to elastic failure than small samples, i.e., the failure stress is smaller in larger samples. The data of Chakrabarti *et al.*[6] also suggest a rather large finite-size effect in the failure stress. This can be interpreted simply by the following argument. The fracture begins near the critical defect. The critical defect in a large sample will be larger, on average, than the critical defect in a small sample and the stress required for failure decreases with increasing defect size. As we will show, the size of the critical defect, $l_{\max}$, scales like $l_{\max} \approx \ln(L)$ where L is the linear dimension of the sample.[5] The breakdown stress σ_f is of order $(1/l_{\max})^{1/\mu}$ where the exponent μ is between 1 and 2. The net result is that $\sigma_f^{\mu} \approx 1/\ln(L)$. The distribution function of breakdown stress $F_L(\sigma)$ has the scaling form[4,5]

$$F_L(\sigma) = 1 - \exp\left[-cL^2 \exp\left[\frac{-k}{\sigma^{\mu}} \right] \right] . \tag{1}$$

We derive this form from a simple scaling argument based on the statistics of percolation clusters and the shape and stress enhancement factor of the critical defect. This form is different from the Weibull distribution[10] form ordinarily used to fit the distribution function of breakdown and failure problems. The Weibull breakdown distribution function is of the form

$$F_L(\sigma) = 1 - \exp(-cL^2 \sigma^m) . \tag{2}$$

A plot of the exponential of an exponential form looks qualitatively similar to a plot of the Weibull form if the Weibull exponent m is large. However, we will show that the exponential of an exponential form fits our numerical data much better than the Weibull form, particularly in the high-reliability limit. Formula (1) is the appropriate distribution function because the size distribution function for cluster sizes in our percolation model is an exponentially decreasing function of cluster size. If the clusters had a power-law distribution function when the Weibull form would be appropriate.

We test all of these theoretical predictions by numerically solving for the equilibrium configuration for a random network of springs placed under a uniform external stress. In our two-dimensional model we use lattice sizes up to $L = 70$ (i.e., 14 700 springs). The numerical results agree with the theoretical predictions. The breakdown stress is a rapidly decreasing function of p near the rigidity percolation threshold, the average breakdown stress is a logarithmically decreasing function of system size, and the exponential of an exponential form for the breakdown-stress distribution function accurately fits the numerical results.

II. LATTICE MODEL

The simple model we use to describe elastic failure is shown in Fig. 1. The nearest-neighbor bonds of a lattice are occupied at random by harmonic springs with probability p. The springs have unit spring constant and have an unstretched length of exactly one lattice spacing. Springs are absent with probability $1-p$. Each spring can withstand a stretch of up to 10^{-4} lattice spacings. If a spring is stretched more than this amount the spring fails completely and irreversibly and is removed from the system. This rather small maximum stretch amount is chosen to keep the force equations approximately linear. The probability is chosen such that p is greater than the rigidity percolation threshold value, p_r. This ensures that the network has a nonzero Young's modulus. Figure 2 shows Young's modulus, E, as a function of the fraction of springs present. Note that E tends to zero at the rigidity percolation threshold $p_r = 0.65 \pm 0.005$.[8] At the rigidity percolation threshold the linear elastic modulus vanishes even though the lattice is still macroscopically connected. This is because external strain can be accommodated completely by the rotation of bonds in the sample without the straining of any springs. If bond-bending forces are present, the rigidity percolation threshold

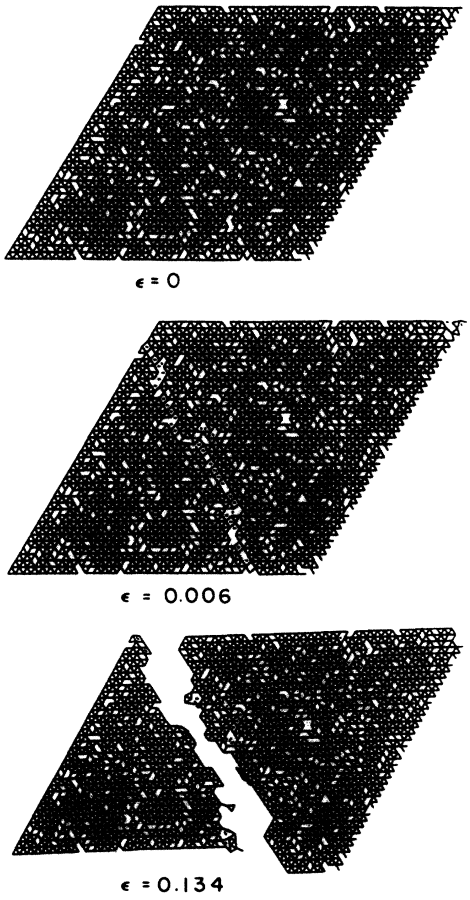

FIG. 1. (a) A random lattice configuration at $p = 0.90$ before the external load is applied. (b) The configuration after rigidity failure has occurred. Note that springs that remain along the failure path, indicated by the incomplete connections, will not be stretched to linear order in the applied strain because they are free to rotate. This results in a zero linear rigidity modulus. (c) The configuration after complete fracture has occurred.

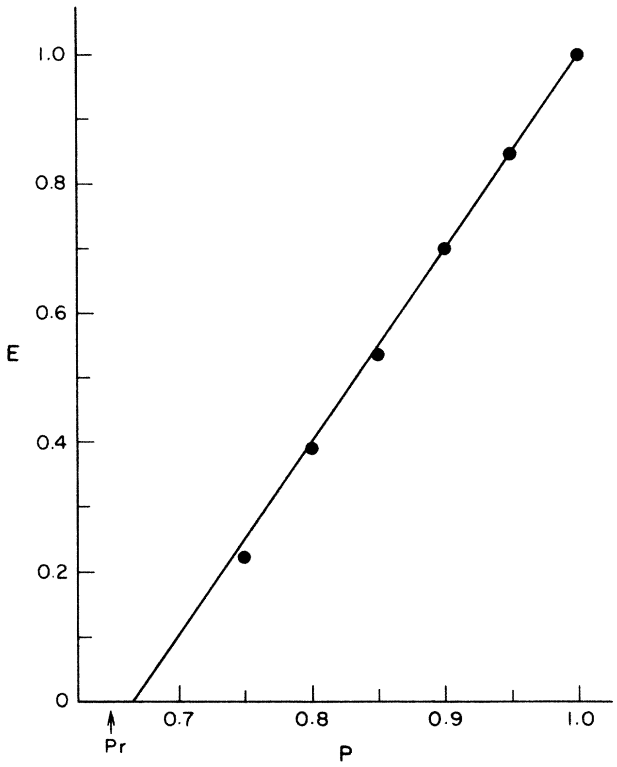

FIG. 2. A plot of Young's modulus $E=\sigma/\epsilon$ [in units of $E(p=1)$] prior to the first failure as a function of p. Note that E tends to zero as p approaches the rigidity percolation threshold at $p=p_r=0.65\pm0.005$. The line is a guide to the eye.

would be moved to the ordinary percolation threshold value[9] p_c ($p_c=0.347$ in the two-dimensional triangular lattice).

This is a simple model of an inhomogeneous elastic medium which is composed of a random mixture of an elastic material and microscopic voids or cracks. The external load on the sample is in the form of a uniform external strain applied to the model in the x direction. Periodic boundary conditions are maintained in the horizontal (x) direction, while the top and bottom surfaces are free.

The initial failure of the material is modeled in the following manner. An external strain, ϵ is applied in the x direction and incremented in units of 0.0005. For each strain, the equilibrium configuration of the system is determined by allowing the system to relax by using the conjugate gradient method.[11] The macroscopic stress, σ, and Young's modulus $E=\sigma/\epsilon$ are then calculated. If one or more springs are strained by more than 10^{-4} then the spring with the largest strain is broken and the system is reequilibrated. This process of breaking and reequilibration continues until no spring is stretched beyond its elastic limit at the current strain. The stress associated with the external strain at which the first spring breaks is called the initial failure stress. The process is continued by incrementing the external strain and re-solving for the equilibrium configuration until the system breaks entirely into two pieces. The breakdown occurs in several steps. These steps can be seen in the stress-strain curve in Fig. 3. The resulting lattice configurations are shown in Figs. 1(b) and 1(c). First, at the stress σ_f which causes the initial failure, a number of springs fail. These springs which fail form a connected path along which no springs are parallel to the applied stress. This results in a dramatic lowering of the elastic modulus. As can be seen in Fig. 3, the linear elastic modulus, $E=\sigma/\epsilon$, vanishes after this initial set of failures. However, the lattice is still connected. As the strain is increased, a nonlinear elastic modulus is observed until a second group of springs fail and again the linear elastic modulus vanishes. This process continues until no connected path exists across the sample. This corresponds to complete fracture of the sample. The first maximum in the stress-strain curve (Fig. 3) is generally higher than all subsequent maxima. If the simulations were performed at constant stress rather than constant strain, the model would fracture immediately after the initial load drop. We will therefore not distinguish between the stress which causes the first load drop and the stress which causes the fracture of the sample.

Inspection of the stress-strain curve (Fig. 3) yields information which is useful in gauging the validity of this type of model for the behavior of brittle materials. For strains below the initial yield drop, the stress-strain curve is linear. Such linearity is expected in real materials at small strain when there is no plastic flow or crack exten-

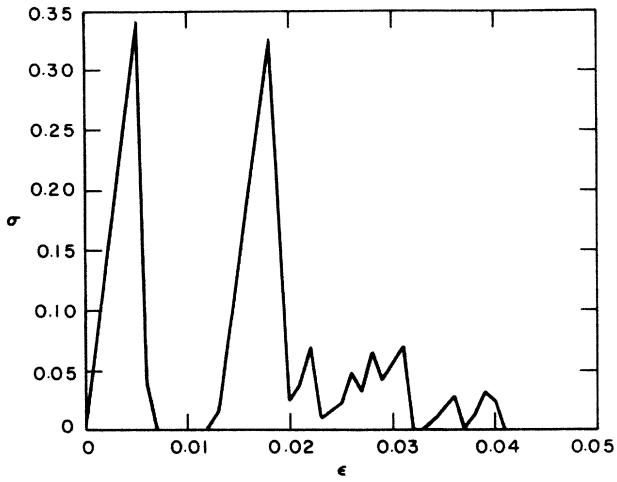

FIG. 3. A plot of the macroscopic stress σ as a function of the applied strain ϵ for a typical sample. The decreasing regions are a result of the breaking of springs in the sample. Notice several things. First, the σ vs ϵ curve is very linear at small ϵ, indicating that the sample has a linear elastic modulus of σ/ϵ. The stress-strain curve prior to the first microscopic failure is linear to an accuracy of 0.1%. Secondly, the rigidity failure begins to occur when the strain is $\epsilon\simeq0.005$ and the external stress is 0.34. A number of springs fail at this external applied stress and the linear elastic modulus tends rapidly to zero. Eventually for strain $\epsilon\simeq0.011$ the elastic modulus becomes nonzero again and several groups of springs break, resulting in another rigidity failure. These types of failure continue far beyond the extent of this figure until the system completely breaks at a strain of $\epsilon=0.134$.

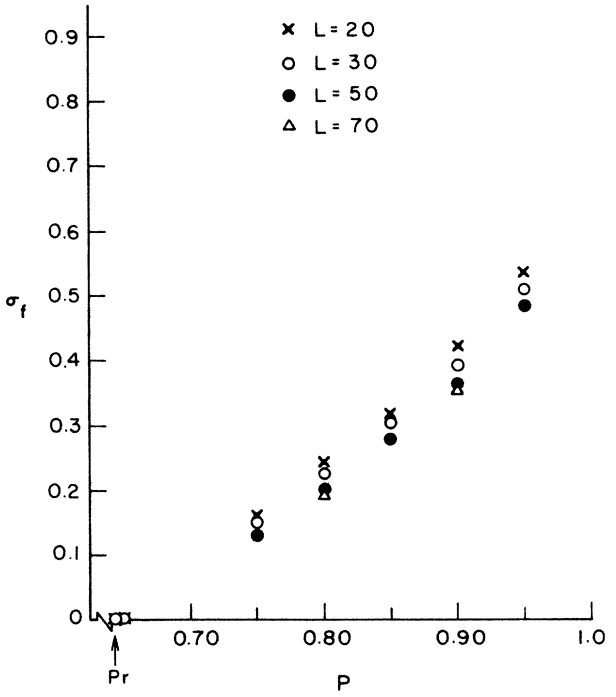

FIG. 4. The failure stress σ_f as a function of p for lattice sizes $L=20$, 30, 50, and 70. Note that at fixed p, σ_f is a slowly decreasing function of L.

sion. While the stress of the system drops to zero in our model following the first stress maximum, real materials do not exhibit zero stress at finite strain prior to failure. The zero-stress regions correspond to periods of spring rotation where no springs are carrying load. This is an artifact of this model which can be rectified by including bond-bening terms in the energy which penalize rotations away from the equilibrium bond angle of 60°. Inclusion of such terms in the rigidity percolation problem moves the rigidity percolation threshold to the ordinary percolation threshold and changes the universality class of the threshold.[9]

In Fig. 4 we show the initial failure stress as a function of spring probability p and system size L. Note that the failure stress is a decreasing function of p as p approaches the rigidity percolation threshold p_r. This effect is caused by the fact that the microscopic voids present in the samples are large for p close to p_r and a few springs are carrying the entire load on the sample.

III. DISTRIBUTION OF FAILURE STRESSES

The initial failure occurs near a particular type of defect configuration. The failure stress depends crucially on the size of these defect configurations. When the defect fraction is close to zero the defect clusters will all be small. This does not imply that the ratio of the failure stress to the failure stress in the perfect system tends to unity as $p \to 1$. On the contrary, even if there is only a single defect in the system the failure stress will be reduced by a finite amount from the value in the pure system. In our model the removal of a single spring oriented along the x direction reduces the initial failure stress by about 20%. Therefore the removal of even a very small number of springs will reduce the initial failure stress by at least 20%.

Figure 4 displays a plot of the initial failure stress σ_f as a function of p for $L=20$, 30, 50, and 70 on a two-dimensional lattice. Note that σ_f tends rapidly to zero as p approaches the rigidity percolation threshold p_r. Note also that the failure stress in Fig. 4 is a slowly decreasing function of the system size L. As in any model in which some quantity depends on the characteristics of the most unusual configurations of a random system, the failure stress in this model displays an intrinsic finite-size scaling behavior.[5] The failure stress is determined by the linear dimension of the critical defect. The critical defect in a random elastic network is a configuration in which two linear cracks almost touch each other. A crack of this type is displayed in Fig. 5. If a single linear crack of length l is placed in a uniform external stress then the stress is enhanced at the tip of the crack by a factor proportional to $(l)^{1/2}$. This is demonstrated in Fig. 6(a). However, if two cracks of length $l/2$ are placed in close proximity to each other so that the distance between the tips of the cracks is much less than $l/2$ then the stress in between the cracks is enhanced by a factor of order l. This is demonstrated in Fig. 6(b). For large isolated defects the stress is much larger between two cracks of length $l/2$ than at the tips of one crack of length l.

The finite-size dependence shown in Fig. 4 is caused by the fact that the critical defect in a large sample will typically be larger than the critical defect in a smaller system. A rough estimate of the L dependence of σ_f can be given as follows. For $1-p \ll 1$ the probability of getting a defect of the type shown in Fig. 5 somewhere in our two-dimensional system is of order $(1-p)^l L^2$. The size of the critical defect is determined by the requirement that there is no defect larger than the critical defect. This implies that $(1-p)^l/L^2$ is of order unity. Therefore the size of the critical defect is given by $l_{\max} \approx -\ln(L)/\ln(1-p)$ for large L.

The dependence of the failure stress on the size of the critical defect is particularly simple for models of dielectric breakdown in metal-loaded dielectrics[3] and Ohmic-

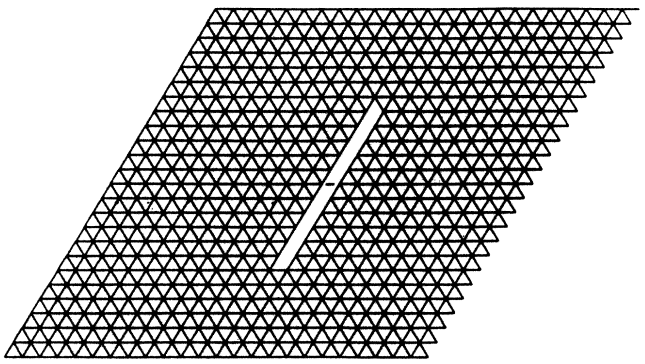

FIG. 5. The configuration we call the critical defect. It is composed of two linear cracks of length l in close proximity oriented perpendicular to the applied stress.

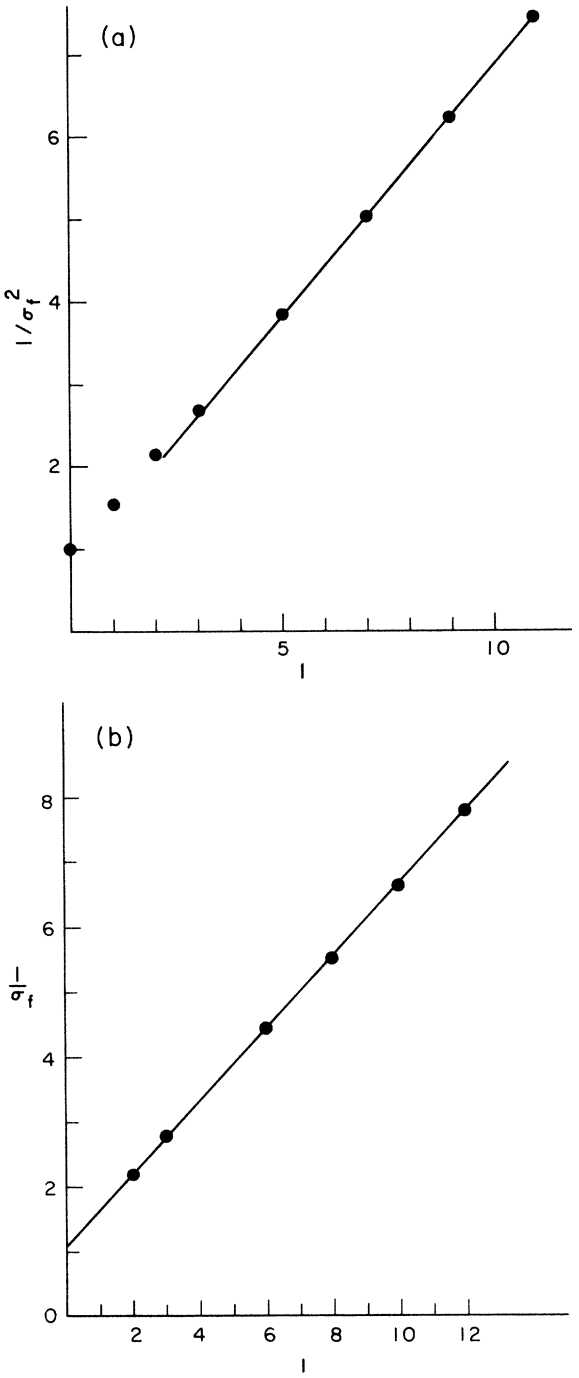

FIG. 6. (a) A plot of $1/\sigma_f^2$ for a defect which is a line of l missing springs oriented perpendicular to the applied stress. Note the linear dependence of $1/\sigma_b^2$ on l. (b) A plot of $1/\sigma_f$ vs the length l of the defect pictured in Fig. 5. Note the linear dependence of $1/\sigma_f$ on l.

heating failures in random networks of conductors and insulators.[4] For the case of dielectric breakdown, the breakdown applied electric field is proportional to the inverse of the linear dimension of the critical defect. The critical defect is a pair of conducting clusters oriented along the applied field. The elastic failure problem is more subtle because of the very slow decay of elastic strain fields. The elastic strain field decays as $1/r^{1/2}$ for distance r away from a single defect. Because of this, single linear defects can contribute significantly to the elastic failure problem even though they do not play a major role in dielectric breakdown or Ohmic failure problems. The failure stress should scale as

$$\sigma_f^{\mu} \approx \frac{1}{l_{\max}} \approx \frac{1}{\ln(L)} . \tag{3}$$

The exponent μ lies somewhere in the range $1 \leq \mu \leq 2$. If nearby pairs of defects dominate the critical defect problem then $\mu=1$. The case $\mu=1$ is found for models of dielectric breakdown and Ohmic-heating failure in random mixtures of conductors and insulators. If isolated defects dominate the critical defect problem then $\mu=2$. Our numerical results are equally consistent with both $\mu=1$ and $\mu=2$.

To show this, in Figs. 7(a) and 7(b) we plot $1/\sigma_f$ ($\mu=1$) and $1/\sigma_f^2$ ($\mu=2$) versus the logarithm of the system size for several different p's. The data in both plots are reasonably consistent with Eq. (3). The slope of the lines is small for p close to unity and large for p close to p_r. From these data we can make the empirical observation that the average initial failure stress σ_b scales like[3,5]

$$\sigma_b^{\mu} \approx \frac{1}{A(p)+B(p)\ln(L)} , \tag{4}$$

where the exponent μ is roughly between 1 and 2. The coefficient $B(p)$ is small for p close to unity and diverges as $p \rightarrow p_r$.

This form for the average failure stress can be derived from the form of the failure stress distribution function. Clearly since the systems being modeled are random, the failure stresses will have some distribution function. Different samples will have different failure stresses. However, there does exist a smooth distribution function for the failure stresses of samples with a given p and L. We will sketch the derivation of the form for this function and show that the result is consistent with the numerical distribution function found from the computer simulations. The details of the derivation can be found in Ref. 5.

The failure stress is determined by the linear size l of the largest defect in the sample. Let $C_L(l_{\max})$ be the probability that no defect larger than size $l_{\max}$ exists in a d-dimensional cubical volume L^d. We then subdivide the cube with volume L^d into $(L/L_1)^d$ smaller cubes of linear dimension L_1. If the characteristic size of the largest defects is much smaller than L_1 then the statistical independence of the subcubes implies that the probability of there being no defect larger than $l_{\max}$ on the L^d lattice is

$$[C_{L_1}(l_{\max})]^{(L/L_1)^d} \approx C_L(l_{\max}) . \tag{5}$$

This, along with the fact that the distribution function for percolation cluster sizes scales like[12] $C_L(n) \approx 1 - cL^2\exp(-kl)$ for large l, we arrive at the result

$$C_L(l_{\max}) = \exp[-cL^2\exp(-kl_{\max})] . \tag{6}$$

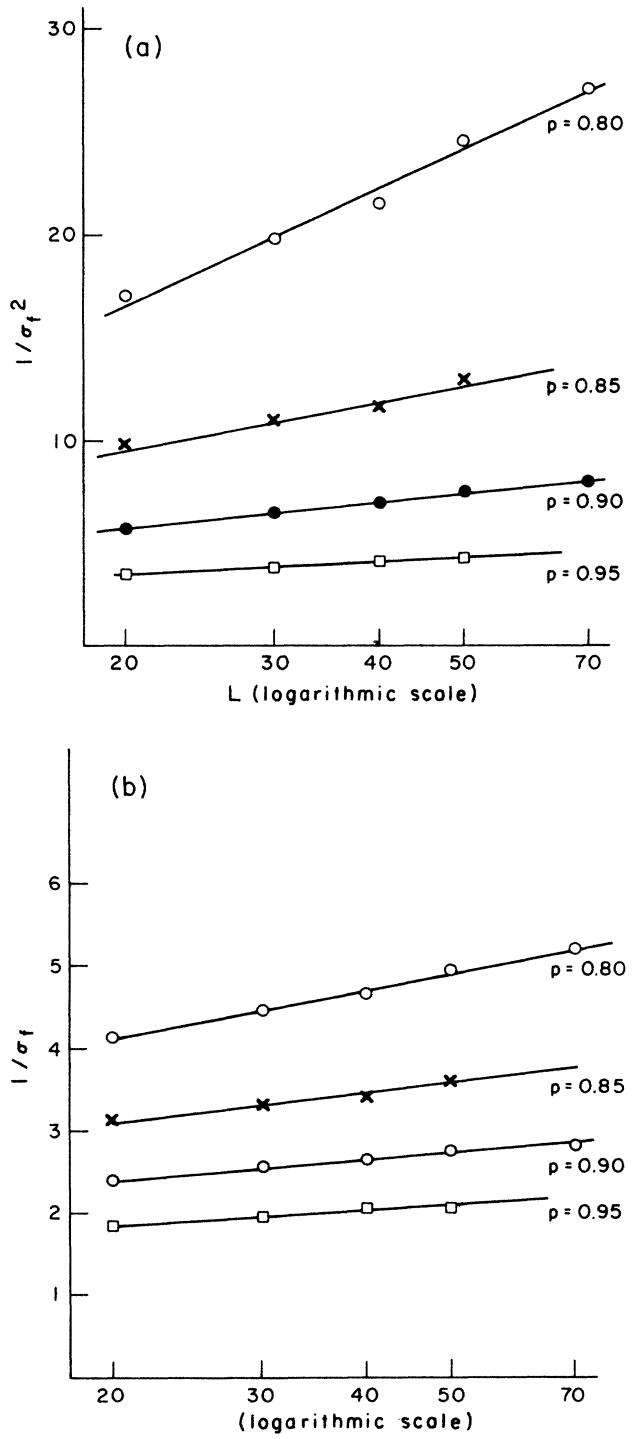

FIG. 7. (a) A plot of $1/\sigma_f^{\mu}$ ($\mu=2$) vs the logarithm of the system size L for several different p's. (b) A plot of $1/\sigma_f^{\mu}$ ($\mu=1$) vs the logarithm of the system size L for several different p's. Note that Eq. (4) fits the data equally well for both $\mu=1$ and $\mu=2$.

This is the form first derived by Duxbury and Leath for a similar problem involving fuse failure in a random system.[5] This distribution function is appropriate as long as p is not too close to the rigidity percolation threshold.

If the probability of finding a defect of size l happened to be an algebraically decaying function (as it will when p is close to the rigidity percolation threshold), $C_L(l)\approx 1-cL^d l^{-m'}$, then the distribution function would be

$$C_L(l_{\max})=\exp(-cL^d l_{\max}^{-m'}) . \tag{7}$$

This distribution function is called the Weibull distribution function and is widely used to fit failure data.[10]

We can use the result (6) to give the distribution function for the elastic failure stress in our model. We argued earlier that the enhancement of the stress in the neighborhood of the critical defect is proportional to $1/l_{\max}^{\mu}$ where $l_{\max}$ is the size of the critical defect and $1\le\mu\le 2$. Therefore the failure stress distribution function $F_L(E)$ is of the form given by Eq. (1),

$$F_L(\sigma)\approx 1-\exp\left[-cL^d\exp\left[-\frac{k}{\sigma^{\mu}}\right]\right] .$$

The function $F_L(\sigma)$ is the probability that a sample of size L will experience an elastic failure if an external stress σ is applied to the sample. Note that for small σ, the probability of failure is very small. The probability tends to unity as $\sigma\to\infty$. The constants k and c are characteristic of microscopic properties of the system. The parameter k vanishes at the rigidity percolation threshold. The connection of this analysis to the logarithmic scaling of the average failure stress (4) can now be made clear. The average failure stress will be close to the value $\sigma_{1/2}$, which is defined as the value of σ for which half of the samples will fail:

$$\tfrac{1}{2}=F_L(\sigma_{1/2})=1-\exp\left[-cL^2\exp\left[-\frac{k}{\sigma_{1/2}^{\mu}}\right]\right] . \tag{8}$$

This can be easily solved for $\sigma_{1/2}$:

$$\sigma_{1/2}^{\mu}=\frac{1}{A(p)+B(p)\ln(L)} , \tag{9a}$$

$$A(p)=\frac{\ln(c)-\ln[\ln(2)]}{k} , \tag{9b}$$

$$B(p)=\frac{2}{k} . \tag{9c}$$

Equation (4) therefore follows from the distribution function (1). The equivalent Weibull distribution function is

$$F_L(\sigma)=1-\exp(-cL^2\sigma^m) , \tag{10}$$

where $m=m'\mu$ and the average failure stress scales as

$$\sigma_{1/2}\approx L^{-2/m} . \tag{11}$$

We will now demonstrate that the form of the failure distribution (1) gives a better fit to the failure distribution function than the Weibull form (10). In Fig. 8(a) we plot the logarithm of the logarithm of the distribution function versus $1/\sigma^{\mu}$ ($\mu=1$). In Fig. 8(b) we plot the same function versus $1/\sigma^{\mu}$ ($\mu=2$) and in Fig. 8(c) we plot the same function versus $-\ln(\sigma)$. If (1) is the appropriate form of the distribution function and we make the correct choice for μ then the data for the two different lattice sizes should collapse onto a single straight line in

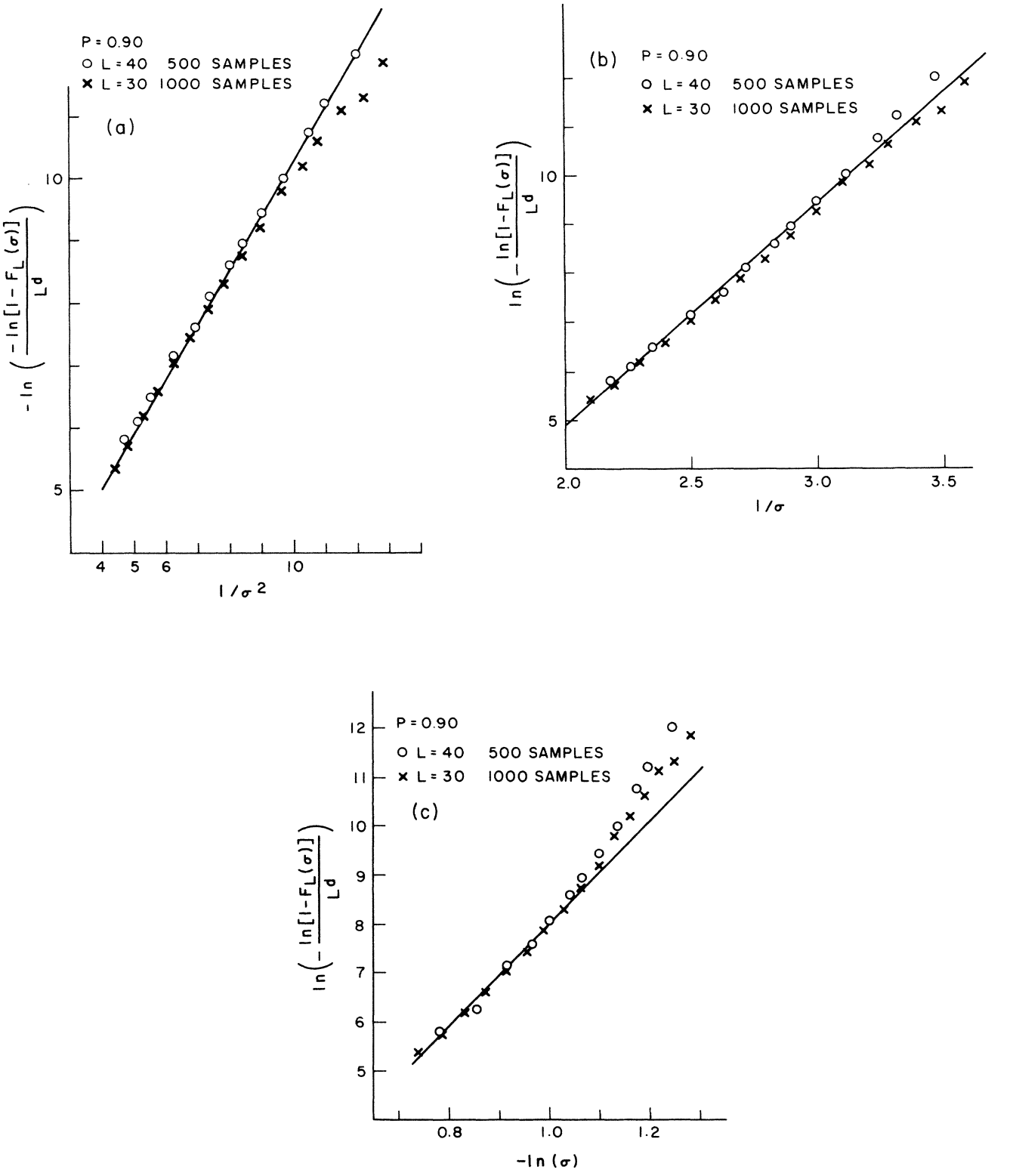

FIG. 8. A plot of the failure probability $F_L(\sigma)$ as a function of σ for two different lattice sizes at $p=0.90$. The data are presented in a manner so that we can differentiate between the Duxbury-Leath form [Eq. (1)] and the Weibull form [Eq. (10)]. In Fig. 8(a) the logarithm of the logarithm of F_L is plotted vs $1/\sigma^{\mu}$ ($\mu=2$). In Fig. 8(b) the logarithm of the logarithm of F_L is plotted vs $1/\sigma^{\mu}$ ($\mu=1$). If (1) is the correct form for the distribution function and we choose the correct value of μ then the data for the two different lattice sizes should collapse onto a single straight line. In Fig. 8(c) the same function of F_L is plotted vs the logarithm of σ. If the Weibull form (10) is appropriate then the data will collapse onto a single straight line. As can be seen, both the $\mu=1$ and $\mu=2$ cases of Eq. (1) fit the data considerably better than Eq. (10).

Fig. 8(a) or 8(b). If the Weibull form (10) is appropriate then the data will collapse to a single straight line in Fig. 8(c). As can be seen, the data form nice straight lines in both figures, 8(a) and 8(b), whereas the data in Fig. 8(c) are noticeably curved. The slope of the guide to the eye in the Weibull plot is the Weibull parameter m. The data indicate that m is quite large ($m \approx 10$). This is a good empirical signal that perhaps (1) may be the more appropriate distribution function.

IV. CONCLUSIONS

These theoretical calculations and scaling arguments can be tested in experimental situations and should apply to a number of different types of random brittle materials; among these would be ceramics, amalgamates, and sintered powders. The important aspect of each of these materials is that they have randomly distributed defects. Based on these theoretical arguments and the numerical data we suggest the following critical experiments. First, the initial failure stress should be measured in a large number of similarly prepared random materials. This should be done as a function of randomness and system size. The resulting distribution functions can be plotted in the manner given in Fig. 8(a) or 8(b) to test the Duxbury-Leath form for the distribution function. The manner in which the average failure stress depends on p and L can be tested against the expected form (4). The Duxbury-Leath (1) form should be the relevant distribution function in cases where the Weibull exponent m is rather large. This would provide an indication that the cluster size distribution function is probably exponential rather than a power law.

ACKNOWLEDGMENTS

We would like to thank Phil Duxbury and Mike Thorpe for useful conversations.

---

*Present address: Department of Materials Science, University of Michigan, Ann Arbor, MI 48109.

[1]A. A. Griffith, Philos. Trans. R. Soc. London Ser. A **221**, 163 (1920).

[2]H. Tada, P. Paris, and G. Irwin, *The Stress Analysis of Cracks Handbook* (Doll Research, St. Louis, 1973); S. M. Weiderhorn, Annu. Rev. Mater. Sci. **14**, 373 (1984); R. W. Davidge, *Mechanical Behavior of Ceramics,* Cambridge Solid State Sciences Series (Cambridge University Press, Cambridge, England, 1979); J. E. Gordon, *The New Science of Strong Materials* (Princeton Unversity Press, Princeton, NJ, 1984).

[3]H. Takayasu, Phys. Rev. Lett. **54**, 1099 (1985); D. R. Bowman and D. Stroud (unpublished); P. D. Beale and P. M. Duxbury, Phys. Rev. B **37**, 2785 (1988).

[4]L. De Archangelis, S. Redner, and H. J. Herrman, J. Phys. Lett. (Paris) **46**, L585 (195); P. M. Duxbury, P. D. Beale, and P. L. Leath, Phys. Rev. Lett. **57**, 1052 (1986).

[5]P. M. Duxbury and P. L. Leath, J. Phys. A **20**, L411 (1987); P. M. Duxbury, P. L. Leath, and P. D. Beale, Phys. Rev. B **36**, 367 (1987).

[6]R. F. Smalley, Jr., D. L. Turcotte, and S. A. Solla, J. Geophys. Res. **90**, 1894 (1985); B. K. Chakrabarti, D. Chowdury, and D. Stauffer, Z. Phys. B **62**, 343 (1986); P. Ray and B. K. Chakrabarti, Solid State Commun. **53**, 477 (1985); P. Ray and B. K. Chakrabarti, J. Phys. C **18**, L185 (1985); M. Sahimi and J. D. Goddard, Phys. Rev. B **33**, 7848 (1986).

[7]S. C. Feng and P. N. Sen, Phys. Rev. Lett. **52**, 216 (1984).

[8]M. A. Lemieux, P. Breton, and A.-M.S. Tremblay, J. Phys. (Paris) Lett. **46**, L1 (1985); S. Feng, M. F. Thorpe, and E. J. Garboczi, Phys. Rev. B **31**, 276 (1985).

[9]L. M. Schwartz, S. Feng, M. F. Thorpe, and P. N. Sen, Phys. Rev. B **32**, 4607 (1985).

[10]W. Weibull, *Fatigue Testing and Analysis of Results* (Pergamon, New York, 1961).

[11]H. R. Schwarz, H. Rutishauser, and E. Stiefel, *Numerical Analysis of Symmetric Matrices* (Prentice-Hall, New York, 1973).

[12]D. Stauffer, Phys. Rep. **54**, 1 (1979); J. W. Essam, Rep. Prog. Phys. **43**, 833 (1980).